

Simulation of Optical Properties of Silicon Solar Cells Textured with Penetrating V -Shaped Grooves

G. G. Untila[^], A. P. Palov, A. Yu. Poroykov, T. V. Rakhimova, Yu. A. Mankelevich, T. N. Kost, A. B. Chebotareva, and V. V. Dvorkin

Skobeltsyn Institute of Nuclear Physics, Moscow State University, Moscow, 119991 Russia

[^]*e-mail: GUntila@mics.msu.su*

Submitted February 22, 2011; accepted for publication March 11, 2011

Abstract—The coefficients of reflection (R), transmission (T), and absorption (A) of light for two wavelengths $\lambda = 1000$ and 1100 nm for silicon wafers that have thicknesses $t = 50, 100,$ and 200 μm and are textured with penetrating V -shaped grooves with various geometries have been calculated; the half-width of groove's base w (10, 20, and 30 μm) and the depth of the groove d ($0 \leq d \leq t$) have been varied. In the case of an increase in the aspect ratio d/w (in the case of $\lambda = 1100$ nm), the absorption curve $A(d/w)$ monotonically ascends from 6.6 to 67.6%, whereas, for $\lambda = 1000$ nm, a nontrivial dependence $A(d/w)$ is observed: the absorption coefficient first increases to 54%, attains then a maximum of 97% at $d/w = 3$, and then decreases at $d > t/2$ for all values of w . This effect of a decrease in absorption with an increase in d/w distinguishes texturing with penetrating grooves from conventional surface texturing. Distributions of angles of deviations of photons in the plane of bottoms of grooves are obtained; these distributions are represented by a set of δ -type functions.

DOI: 10.1134/S1063782611100228

1. INTRODUCTION

The main problem in photovoltaic industry consists in the necessity of reducing the cost of electrical energy produced by solar cells (SCs). In order to attain this goal, it is necessary to simultaneously solve two contradictory problems.

On the one hand, it is necessary to increase the efficiency of SCs; in particular, European Photovoltaic Industry Association (EPIA) predicted an increase in the efficiency of SCs made of single-crystalline (multicrystalline) silicon from 16.5 (14.5) to 20% (18%) by 2020. On the other hand, it is necessary to reduce the cost of SCs. At present the cost of starting silicon wafers amounts to more than half of the price of a silicon solar module [2]; therefore, there is a tendency to transition to thinner layers of multicrystalline silicon (the EPIA plans to reduce the thickness of silicon SCs to 100 μm by 2020) obtained from inexpensive and, correspondingly, lower-quality raw materials, in particular, metallurgical-grade silicon with a high-level purification [3]. This material features a short diffusion length of nonequilibrium charge carriers, which brings about a decrease in the efficiency of SCs fabricated using traditional structures and technologies. It is due to this that interest has been recently aroused in the development of new SC structures and technologies that could ensure a high efficiency of SCs based on low-quality silicon.

In order to overcome the problems caused by a short diffusion length, an SC structure with a penetrating emitter [4] in the shape of parallel deep vertical

grooves was suggested more than 30 years ago. Progress in this line of research markedly intensified after theoretical calculations [5], which showed that a penetrating emitter has an advantage over a planar one (the calculation was carried out for a radial p - n junction). Experimentally the penetrating emitter was formed, in particular, by chemical etching of deep pores (porous silicon) [6] and also by forming an array of various three-dimensional (3D) structures, i.e., pillar, wire [7], and whiskers [8], using different methods: laser [9] and chemical [10] etching, a vapor-liquid-solid (VLS) procedure [11, 12], and reactive ion etching [12, 13].

However, formation of a penetrating emitter brings about an increase in the area of the p - n junction and, correspondingly, an increase in recombination currents (proportional to the area): at the area itself, in the emitter, and in the space-charge region (SCR). As a result, even at high short-circuit currents J_{sc} , low open-circuit voltages U_{oc} are obtained, for example, $U_{oc} = 544$ mV at $J_{sc} = 37$ mA/cm² [10] and a mere $U_{oc} = 507$ mV at $J_{sc} = 39.2$ mA/cm² [9]. Special study [12] showed that the value of U_{oc} decreases by 61 mV when the area is increased tenfold. Therefore, if the negative effect of an increase in the area of a p - n junction is taken into account, two-dimensional (2D) structures (grooves, walls) [14, 15] can be found to be preferable compared to 3D ones (pores, pillars).

Texturing of the SC surface is a necessary technological operation in fabrication of present-day and next-generation SC structures [16–18]. Texturing is

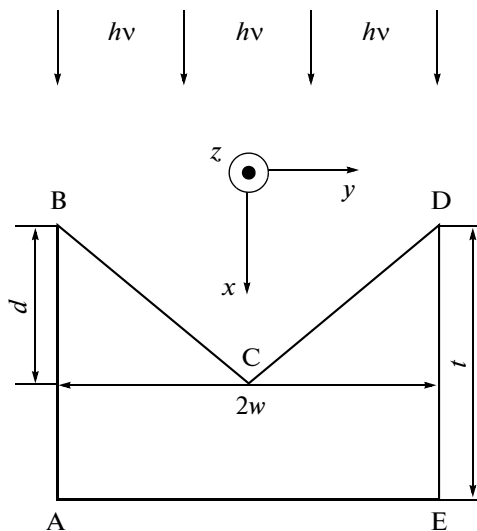


Fig. 1. Geometry of the structure to be simulated.

bound to provide an increase in the absorption coefficient for light (A) due to a decrease in the coefficients of reflection (R) and transmission (T). The latter is decreased by efficient redirection of incident radiation, predominantly along the SC surface. This effect ensures an increase in the length of the optical path and a smaller distance between the region of generation of electron–hole pairs and the emitter, thus increasing the long-wavelength sensitivity [19, 20], which also makes it possible to reduce the requirements imposed on the quality of initial crystalline silicon. Finally, an increase in the angle of entering of radiation into the SC bulk is conducive to total internal reflection of light from the rear surface and, thus, gives rise to the effect known as “capture of light.”

Optical properties of the textured SC surface were simulated for various topologies and geometric forms of structures on silicon [21–23]. Sometimes, even irregularity of texture was taken into account in the course of simulation by introducing special correcting randomizing functions [24–26]. However, analysis of available publications shows that, in the case of a penetrating emitter, optical properties have not been simulated, since the height of pyramids was assumed to be fixed and much smaller than the SC thickness in studies of the effect of the aspect ratio, for example, for various pyramids (conical, hexagonal, quadratic, and triangular) [23]. In contrast, in the case of a penetrating emitter, the depth of the structures is comparable to the SC thickness and, therefore, the previously obtained results cannot be used.

The aim of this study was to fill this gap in knowledge; in particular, we studied the optical properties (reflection, transmission, and absorption) of silicon SCs with the surface textured with V-shaped grooves [27] in relation to the aspect ratio of the grooves and the thickness of the silicon wafer. The choice of such a

form of the structures is caused by the fact that this form brings about a minimal increase in the area of the SC surface. Structures of this type are fabricated, for example, by the method of mechanical texturing with a system of coaxial abrasive discs or by wire cutting [28–30].

2. A MODEL FOR CALCULATION OF OPTICAL PROPERTIES OF A SILICON SOLAR CELL WITH V-SHAPED GROOVES

Reflection, refraction, and absorption of light rays were simulated according to the scheme represented in Fig. 1. The upper SC surface exhibits a profile periodic in the y direction and propagating to infinity in the z direction, which makes the problem of calculation of optical characteristics two-dimensional. Periodic boundary conditions were used at the AB and DE boundaries. The function of distribution of incident rays over angles at the entrance to the region under consideration was specified by a δ function with the angle 0° relative to the x axis. The complex refractive index in the first medium (vacuum) was assumed to be equal to unity ($m_1 = n_1 - ik_1 = 1$), while, in the second medium (silicon), we have $m_2 = n_2 - ik_2$, where the absorption index is defined by the formula

$$k_2 = \frac{\kappa\lambda}{4\pi}; \quad (1)$$

here, κ is the absorption coefficient expressed in nm^{-1} , n_2 is the refractive index, and λ is the wavelength of light expressed in nanometers. Since $n_2 \gg k_2$ for silicon in the wavelength range under study, we used a model of two nonabsorbing media for description of the interface between two media, while the absorption coefficient in silicon was used only in description of losses of radiation within the wafer. All calculations were carried out in the approximation of linear optics, since the wavelengths under study were at least 50 times smaller than geometric sizes of the region involved in calculations.

The aim of optimization was to obtain the maximum coefficient of absorption of infrared photons in a silicon wafer with modified surface. Optimization was carried out over two parameters: over half-width of the groove w and over its aspect ratio d/w , which was assumed to be equal to the ratio of the groove depth d and its half-width w .

All calculated relations for unpolarized light were taken from the theory of classical optics. In the case of incidence of the light ray onto the internal boundary of the wafer, we simulated total internal reflection for angles larger than θ_c calculated from the expression

$$\sin\theta_c = \frac{n_2}{n_1}. \quad (2)$$

For the silicon—vacuum interface, the value of this parameter is $\theta_c = 16.27^\circ$ (16.4°) for the wavelengths of 1000 nm (1100 nm).

The total reflection coefficient for the studied range of wavelengths was calculated as the arithmetic average of reflection coefficients obtained for N starting positions of the ray uniformly distributed at $x = 0$ over y in the range $0-y_{\max}$:

$$R_{\text{tot}} = \frac{1}{N} \sum_{j=1}^N R(y_j). \quad (3)$$

3. ALGORITHMS OF CALCULATIONS

For simulation of reflection, refraction, and absorption of light, we used the method of tracing the rays. One thousand initial rays started parallel to the x axis from positions uniformly distributed over the segment BD. A minimal intensity at which tracking of the ray trajectory was stopped was specified in the range of 0.001–0.0001 in order to ensure calculation of the transmission and reflection with an accuracy of four significant digits.

In the case of transmission through an interface between two media, we generated two rays, except for the cases of total internal reflection. The reflected ray was considered as the primary one, while the refracted ray was always considered as the secondary one. Tracking of rays' trajectories was stopped, first, when the ray left the region under consideration and, second, when the intensity of the ray became lower than a specified minimum. In the case of multiple passage of the ray through the interface, we formed an array of parameters for secondary rays. After simulation of the trajectory of the first ray was terminated, we simulated the trajectories of the second, third, etc., rays until the number of rays in the array reduced to zero; we used parts of the software packages developed earlier by Palov et al. [31–33]. The simulation was carried out for two wavelengths of light, 1000 and 1100 nm, for which the results of calculations are maximally sensitive to the length of optical path of light in the wafer. The typical number of rays taken into account for each starting ray with the wavelength 1000 nm and minimal relative intensity 0.001 was two or three and was nine or ten for the wavelength of 1100 nm.

4. RESULTS AND DISCUSSION

4.1. Effect of the Thickness of Silicon Wafer on Optical Coefficients

Figure 2 illustrates the formation of the reflection R , transmission T , and absorption A coefficients in relation to the aspect ratio for three thicknesses of the wafers: $t = 200$, 100, and 50 μm . Calculations were carried out for the half-width of the groove $w = 10$ μm and for the light with the wavelength $\lambda = 1000$ nm. In calculations the depth of a groove was varied from zero

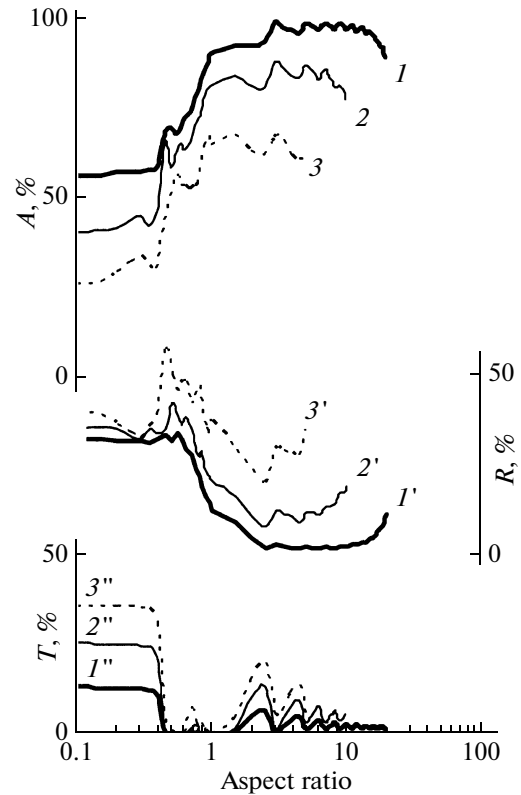


Fig. 2. Dependences of coefficients of absorption A ($1, 2, 3$), reflection R ($1', 2', 3'$), and transmission T ($1'', 2'', 3''$) in a silicon wafer on the aspect ratio of V-shaped grooves with a half-width of 10 μm for the wavelength of light $\lambda = 1$ μm and three thicknesses of the wafer: $t = 200$ μm ($1, 1', 1''$), 100 μm ($2, 2', 2''$), and 50 μm ($3, 3', 3''$).

to wafer's thickness; in the latter case, the bottom of the groove reaches the rear side. Therefore, for wafers with a thickness of 200, 100, and 50 μm , the maximal aspect ratio equals 20, 10, and 5, respectively.

It can be clearly seen from Fig. 2 that texturing with penetrating V-shaped grooves makes it possible to significantly increase the absorption of light. We note that a drastic decrease in the transmission coefficient and a corresponding variation in remaining parameters occur at the aspect ratio ~ 0.4 .

This effect has a simple physical meaning. A ray of light, which falls from vacuum on groove's wall, is refracted and is incident on the rear surface at some angle. If this angle is no smaller than $\arcsin(1/n_2)$, total internal reflection takes place. The value of the aspect ratio for a groove $(d/w)^*$ at which the angle of incidence of the ray on the rear surface is equal to the angle of total internal reflection can be calculated using the formula

$$(d/w)^* = n_2 \cos\left(\arcsin\frac{1}{n_2}\right) \quad (4)$$

and amounts to 0.412 (0.417) for $\lambda = 1000$ nm (1100 nm).

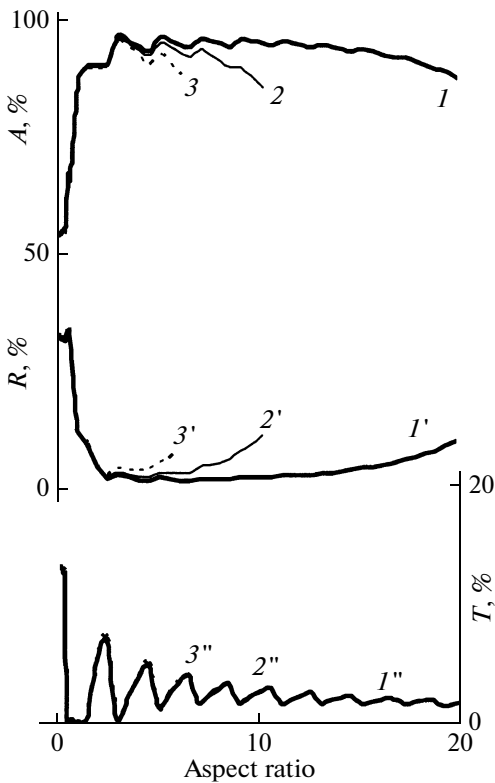


Fig. 3. Dependences of coefficients of absorption A (1 , 2 , 3), reflection R ($1'$, $2'$, $3'$), and transmission T ($1''$, $2''$, $3''$) for a silicon wafer on the aspect ratio of V-shaped grooves for the wavelength of incident light $\lambda = 1 \mu\text{m}$ and three values of the half-width of the groove: $w = 10 \mu\text{m}$ (1 , $1'$, $1''$), $20 \mu\text{m}$ (2 , $2'$, $2''$), and $30 \mu\text{m}$ (3 , $3'$, $3''$).

At a thickness of $200 \mu\text{m}$, absorption increases by 1.8 times from 54 to 97% even at the aspect ratio $d/w = 3$. Since 97% of light with the wavelength of $1 \mu\text{m}$ is absorbed in the silicon layer with the thickness of $530 \mu\text{m}$, we find that the effective path length of light L_{opt} in the wafer is by 2.65 times larger than wafer's thickness. In the range of $d/w = 3$ –10, absorption is practically constant, while, at $d/w > 10$ (i.e., when the depth of the groove exceeds the half-thickness of the wafer) absorption decreases: it is equal to 87% at $d/w = 20$, in which case the bottom of the groove reaches the rear side. The decrease in absorption occurs due to an increase in reflection, since total internal reflection is mainly observed at the rear surface, which is physically understandable.

Systematic features are qualitatively identical for thicknesses of 100 and $50 \mu\text{m}$: as the value of d/w is increased, absorption at $t = 100 \mu\text{m}$ ($50 \mu\text{m}$) increases first by 2.2 (2.7) times from 39 (24) to 86% (65%), i.e., the effective path length of light is 3 (3.3) times larger than the wafer thickness. When the bottom of the groove intersects the middle of the wafer thickness, absorption decreases and attains 69% (59%) at a maximum value of d/w .

4.2. Effect of the Width of a V-Shaped Groove on Optical Coefficients

We studied the effect of the half-width of the base of a V-shaped groove on optical coefficients by measuring their dependence on the aspect ratio for three values of w : 10, 20, and $30 \mu\text{m}$ (Fig. 3).

Simulation showed that, at identical aspect ratios, the calculated coefficients of transmission of light with $\lambda = 1000 \text{ nm}$ remain practically unchanged in the case wherein the half-width of the base of a groove is varied in the range from 10 to $30 \mu\text{m}$. The highest absorption is observed at $d/w = 3$ for all three curves; an increase in absorption (and, correspondingly, a decrease in reflection) set in when the bottom of the groove intersects the middle of the wafer. At a maximal value of d/w equal to 20, 10, and 6.7 (for groove's half-widths of 10, 20, and $30 \mu\text{m}$, respectively), the optical parameters of structures are practically identical.

4.3. Comparison of Optical Coefficients for Wavelengths of 1000 and 1100 nm

The refraction coefficient of silicon for the wavelength 1000 nm equals 3.57, and the absorption coefficient is equal to 64 cm^{-1} ; at the same time, for the wavelength 1100 nm, the coefficients equal 3.54 and 3.5 cm^{-1} , respectively. Only the difference between the absorption coefficients is essential; it is this difference that gives rise to different behavior of the reflection and transmission coefficients calculated for a silicon wafer with the thickness $200 \mu\text{m}$ and V-shaped grooves with half-width $10 \mu\text{m}$.

As can be seen from Fig. 4, the coefficients R and T for $\lambda = 1100 \text{ nm}$ significantly exceed the corresponding coefficients for $\lambda = 1000 \text{ nm}$. In addition these dependences radically differ from each other in relation to the dependence on the aspect ratio. In the case of $\lambda = 1000 \text{ nm}$, reflection drastically decreases even at an aspect ratio equal to 3 and then starts to slowly increase at $d/w > 10$, whereas, at $\lambda = 1100 \text{ nm}$, reflection continues to decrease until the maximum value of d/w is attained.

The behavior of the curves of absorption of light also greatly differs. For $\lambda = 1000 \text{ nm}$, absorption attains a maximum at $d/w = 3$ and then decreases at $d > t/2$, whereas, for $\lambda = 1100 \text{ nm}$, absorption increases tenfold from 6.6% at $d/w = 0$ to 67.6% at $d/w = 20$ and evidently does not attain a maximum.

4.4. Distribution of Angles of Deflection of Photons in the Case of Multiple Reflections

An interesting fact is the observed periodicity of the R and T coefficients with the period of the aspect ratio equal approximately to 2. In order to study this phenomenon, we calculated the angular distribution of photons with the wavelength 1100 nm as a function of modulus of the angle of deflection from the x axis in

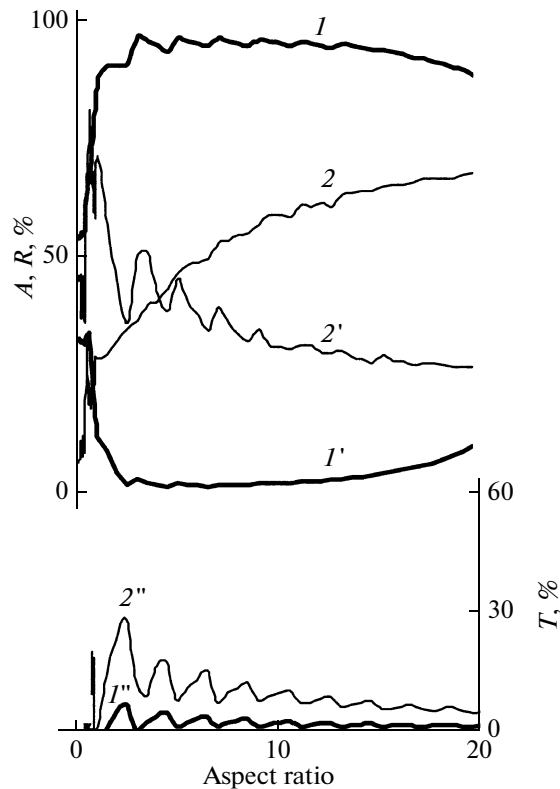


Fig. 4. Dependences of the coefficients of absorption A ($1, 2$), reflection R ($1', 2'$), and transmission T ($1'', 2''$) in a silicon wafer on the aspect ratio of V-shaped grooves for the wavelength of incident light $\lambda = 1 \mu\text{m}$ ($1, 1', 1''$) and $1.1 \mu\text{m}$ ($2, 2', 2''$).

the plane of grooves' bottom. The results of calculations for the aspect ratios equal to unity and 2 are shown in Fig. 5.

For the aspect ratio equal to unity, the angular distribution includes only two appreciable peaks: the first peak corresponds to the angle of refraction of the ray at the vacuum–silicon interface, and the second peak is related to reflection of the ray from the vacuum–silicon interface with subsequent refraction at the vacuum–silicon interface. In both cases the angle of deflection exceeds the value of the critical angle (16°) for total internal reflection at the silicon–vacuum interface. As a result we have total internal reflection and, as a consequence, a minimal coefficient of transmission and a maximal coefficient of reflection. It is worth noting that the width of the peaks in the angular distribution of photons is determined only by the step in the grid of calculations over the angles of deflection of photons; in the case under consideration, this width was 1° .

For the aspect ratio equal to 2, a perceptible number of photons (namely, 28%) have the deflection angle smaller than the critical one, which was responsible for an increase in T and a decrease in R at $d/w = 2$.

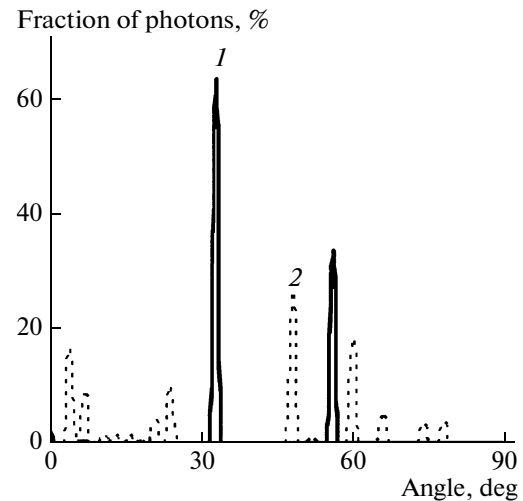


Fig. 5. Angular distribution of photons with respect to the x axis in the plane of the bottom of V-shaped grooves at the aspect ratios $d/w = 1$ (1) and 2 (2). The wavelength of light $\lambda = 1100 \text{ nm}$, the thickness of the silicon wafer $t = 200 \mu\text{m}$, and the half-width of the groove $w = 10 \mu\text{m}$.

5. CONCLUSIONS

We simulated the coefficients of reflection, transmission, and absorption of photons with the wavelengths of 1000 and 1100 nm for silicon wafers with thicknesses of 50, 100, and 200 μm and with the front surface textured with V-shaped penetrating grooves and with the smooth rear surface. At a fixed value of the half-width of the base of a groove w (10, 20, or 30 μm), the depth of the groove d was varied in the range from zero to the maximal possible value equal to wafer's thickness, which caused a variation in the aspect ratio d/w for the groove. We detected important systematic features in the behavior of the reflection, transmission, and absorption coefficients during the above-mentioned variation in the geometry of a sample.

For the wavelength of light $\lambda = 1100 \text{ nm}$, absorption steadily increases from 6.6 to 67.6% as the aspect ratio is increased from $d/w = 0$ to the maximal value $d/w = 20$, whereas, for the wavelength $\lambda = 1000 \text{ nm}$, the dependence $A(d/w)$ passes through a maximum. As a rule the maximal value of the absorption coefficient is attained at the aspect ratio $d/w = 3$ and starts to decrease in the case wherein the groove's bottom intersects the middle of the wafer. This effect could be expected since, in the case of penetrating grooves, an increase in their depth brings about a considerable decrease in the volume of absorbing silicon; this volume halves at the limit of the largest aspect ratio. It is worth noting that, in the case in which the aspect ratio was increased due to a decrease in the width of the base of the groove at its fixed height, a maximum in the curves $A(d/w)$ was not observed [23]. Thus, apparently, it is this cause of a decrease in absorption with an increase in the aspect ratio, as observed for the wavelength of light 1000 nm, which represents a distinctive

property of textured penetrating grooves in comparison with conventional surface texturing, in which case the height of textured structures was much smaller than the thickness of the silicon wafer.

It is also a useful result that similarly large absorption of light (97% at a wavelength of 1000 nm) can be obtained using grooves with different widths (10, 20, and 30 μm) if the aspect ratio $d/w \approx 3$ in this case.

It is evident that a decrease in the thickness of a wafer brings about a decrease in the absorption of light. However, the effect of an increase in the length of optical path of light L_{opt} in thin wafers is even more pronounced than in thick films. For example, for a wafer with the thickness $t = 200 \mu\text{m}$, the ratio L_{opt}/t amounts to 2.65, whereas, at $t = 100 \mu\text{m}$, this quantity increases to 3 and attains the value of 3.3 at $t = 50 \mu\text{m}$.

It is found that, at $d/w > 1$, the curves $T(d/w)$ and $R(d/w)$ exhibit a pulsed component with a period of $d/w = 2$; in this case the reflection and transmission coefficients are varied in antiphase. Possibly this effect is related to angular distribution in deflections of photons in the plane of the grooves' base; this distribution is represented by a set of δ functions. Such a form of these distributions is basically possible in a linear texture, in which case the plane of propagation of photons remains unchanged, while the direction of photons' propagation varies discretely.

Since $A(d/w)$ features a maximum at $\lambda = 1000 \text{ nm}$ and monotonically increases in the case of $\lambda = 1100 \text{ nm}$, then, in order to optimize the aspect ratio of grooves with the aim of maximization of absorption in a silicon solar cell, it is necessary to carry out corresponding calculations in the entire range of spectral sensitivity of solar cells; this will be the subject of our next publication.

ACKNOWLEDGMENTS

We thank A.F. Yaremchuk for valuable discussions in the course of preparation of this publication.

This study was supported by the Ministry of Education and Science of the Russian Federation (State Contract no. 02.740.11.0055) in the framework of the program "State Support of Leading Scientific Schools" (grant no. NSh-3322.2010.2) and was also supported by the Russian Foundation for Basic Research (project no. 10-08-01171).

REFERENCES

- G. P. Willeke, in *Proceedings of the 19th European Photovoltaic Solar Energy Conference* (Paris, France, 2004), p. 1.
- R. Einhaus, D. Sarti, S. Pleier, M. Blum, P. J. Ribeyron, and F. Duran, in *Proceedings of the 116th European Photovoltaic Solar Energy Conference* (Glasgow, UK, 2000).
- V. Hoffmann, K. Petter, J. Djordjevic-Reiss, E. Enebakk, J. T. Hakedal, R. Tronstad, T. Vlasenko, I. Buchovskaja, S. Beringov, and M. Bauer, in *Proceedings of the 23rd European Photovoltaic Solar Energy Conference* (Valencia, Spain, 2008), p. 1117.
- J. Lindmayer and C. Wrigley, in *Proceedings of the 12th IEEE Photovoltaic Special Conference* (1976), p. 1:30.
- B. M. Kayes, H. A. Atwater, and N. S. Lewis, *J. Appl. Phys.* **97**, 114302 (2005).
- H. J. Lewerenz, M. Aggour, T. Stempel, M. Lublow, J. Grzanna, and K. Skorupska, *J. Electroanal. Chem.* **619–620**, 137 (2008).
- K.-Q. Peng and S.-T. Lee, *Adv. Mater.* **20**, 1 (2010).
- K.-P. Kim, S. Li, H.-K. Lyu, S.-H. Woo, S. K. Lim, D. Chang, H. S. Oh, and D.-K. Hwang, *Jpn. J. Appl. Phys.* **49**, 056503 (2010).
- V. V. Iyengar, B. K. Nayak, and M. C. Gupta, *Sol. Energy Mater. Sol. Cells* **94**, 2251 (2010).
- D. Kumar, S. K. Srivastava, P. K. Singh, M. Husain, and V. Kumar, *Sol. Energy Mater. Sol. Cells* (2010). doi.org/10.1016/j.solmat.2010.04.024
- M. D. Kelzenberg, S. W. Boettcher, J. A. Petykiewicz, D. B. Turner-Evans, M. C. Putnam, E. L. Warren, J. M. Spurgeon, R. M. Briggs, N. S. Lewis, and H. A. Atwater, *Nature Mater.* **9**, 239 (2010).
- B. M. Kayes, M. A. Filler, M. D. Henry, J. R. Maiolo, M. D. Kelzenberg, M. C. Putnam, J. M. Spurgeon, K. E. Plass, A. Scherer, N. S. Lewis, and H. A. Atwater, in *Proceedings of the 33th Photovoltaic Special Conference* (San Diego, CA, 2008).
- H. P. Yoon, Y. A. Yuwen, C. E. Kendrick, G. D. Barber, N. J. Podraza, J. M. Redwing, T. E. Mallouk, C. R. Wronski, and T. S. Mayer, *Appl. Phys. Lett.* **96**, 213503 (2010).
- D. L. Kendall, *Appl. Phys. Lett.* **25**, 195 (1975).
- E. V. Astrova and G. V. Fedulova, *J. Micromech. Microeng.* **19**, 095009 (2009).
- U. Gangopadhyay, S. K. Dutta, and H. Saha, *Texturization and Light Trapping in Silicon Solar Cells* (Nova Science, New York, 2009).
- M. Halbwx, T. Sarnet, Ph. Delaporte, M. Sentis, H. Etienne, F. Torregrosa, V. Vervisch, I. Perichaud, and S. Martinuzzi, *Thin Solid Films* **516**, 6791 (2008).
- M. Abbott and J. Cotter, *Progr. Photovolt.: Res. Appl.* **14**, 225 (2006).
- J. C. Zolper, S. Narayanan, S. R. Wenham, and M. A. Green, *Appl. Phys. Lett.* **55**, 2363 (1989).
- A. Poroykov, G. Untila, T. Kost, A. Chebotareva, M. Timofeyev, M. Zaks, A. Sitnikov, O. Solodukha, O. Novodvorsky, E. Khaydukov, and D. Zuev, in *Proceedings of the 25th European Photovoltaic Solar Energy Conference* (Valencia, Spain, 2010), p. 2584.
- Z. Xiong, F. Zhao, J. Yang, and X. Hu, *Appl. Phys. Lett.* **96**, 181903 (2010).
- T. Yagi, Y. Uraoka, and T. Fuyuki, *Sol. Energy Mater. Sol. Cells* **90**, 2647 (2006).
- X.-S. Hua, Y.-J. Zhang, and H.-W. Wang, *Sol. Energy Mater. Sol. Cells* **94**, 258 (2010).
- D. Dominé, F.-J. Haug, C. Battaglia, and C. Ballif, *J. Appl. Phys.* **107**, 044504 (2010).
- K. Jäger and M. Zeman, *Appl. Phys. Lett.* **95**, 171108 (2009).

26. K. Jäger, O. Isabella, L. Zhao, and M. Zeman, *Phys. Status Solidi C* **7**, 945 (2010).
27. Y. G. Xiao, M. Lestrade, Z. Q. Li, and Z. M. S. Li, *Proc. SPIE* **6651** (2007).
28. G. Willeke, H. Nussbaumer, H. Bender, and E. Bucher, *Sol. Energy Mater. Sol. Cells* **26**, 345 (1992).
29. H. Bender, J. Szlufcik, H. Nussbaumer, G. Palmers, O. Evrard, J. Nijs, R. Mertens, E. Bucher, and G. Willeke, *Appl. Phys. Lett.* **62**, 2941 (1993).
30. M. Spiegel, C. Gerhards, F. Huster, W. Jooss, P. Fath, and E. Bucher, *Sol. Energy Mater. Sol. Cells* **74**, 175 (2002).
31. A. P. Palov, V. V. Pletnev, and V. G. Telkovski, *Vacuum* **44**, 901 (1993).
32. A. Palov, H. Fujii, and S. Hiro, *Jpn. J. Appl. Phys.* **37**, 6170 (1998).
33. A. P. Palov, Yu. A. Mankelevich, T. V. Rakhimova, and D. Shamiryan, *J. Phys. D: Appl. Phys.* **43**, 075203 (2010).

Translated by A. Spitsyn